

Developing Mechanistic Understanding of Granular Behaviour in Complex Moving Geometry using the Discrete Element Method. Part A: Measurement and Reconstruction of Turbula[®] Mixer Motion using Positron Emission Particle Tracking

M. Marigo^{1,2}, D. L. Cairns¹, M. Davies¹, M. Cook³
A. Ingram^{2,4,5} and E. H. Stitt¹

Abstract: In this work the complex motion of the Turbula[®] mixer has been measured by Multiple-Positron Emission Particle Tracking (Multiple PEPT) in order to set-up a DEM numerical model. Positron emitting radioactive tracers were attached to three of the pivot bearings on the shaft of the mixer to enable the rotation and translation of the mixer chamber to be tracked in the PEPT camera. The measured movement was mathematically reconstructed and imported into DEM in order to apply the same movement to the modelled vessel.

The three-dimensional motion of particles in a vessel located in the Turbula mixer was then calculated using Discrete Element Modelling (DEM). The DEM code used in this work is a commercially available package provided by DEM-Solutions (EDEM).

Good qualitative agreements have been found between the DEM simulations and experimental data from the literature for the degree of segregation in bi-disperse particle mixtures at long mixing times.

Keywords: Turbula mixer, particle mixing, PEPT, granular blending, DEM.

¹ Johnson Matthey Technology Centre, P.O. Box 1, Belasis Avenue, Billingham, Cleveland, TS23 1LB, United Kingdom

² Centre for Formulation Engineering, Chemical Engineering, School of Engineering, The University of Birmingham, B15 2TT, United Kingdom

³ DEM Solutions, Edinburgh, EH2 3NH, United Kingdom

⁴ Positron Imaging Centre, School of Physics and Astronomy, The University of Birmingham, B15 2TT, United Kingdom

⁵ Corresponding author. Tel.: (+44) (0) 121 414 4548; fax: (+44) (0) 121 414 5324; E-mail: a.ingram@bham.ac.uk.

1 Introduction

The mixing of particles is an important operation in many industries such as, pharmaceutical, food, chemical, metallurgical, ceramic, mineral, cement and food industries as kilns, mixers, dryers and processing granular materials. Understanding and controlling of the mixing mechanisms is fundamental towards achieving the desired characteristics for a final product.

In recent years the advances in computational power has made Discrete Element Method (DEM) a powerful tool for studying systems that involve particulate materials. The Discrete Element Method algorithm was originally presented by [Cundall and Strack (1979)]. After this first work many other DEM simulations have been published in the literature studying the modelling of granular material systems. The motion of particles in rotating blenders such as, drum, double cone, beads mill and V-mixer has been extensively studied and modelled as reported in [Moakher, Shinbrot and Muzzio (2000); Kuo, Knight, Parker, Tsuji, Adams and Seville (2002); Lemieux, Léonard, Doucet, Leclaire, Viens, Chaouki and Bertrand (2008); Liu Xiaoxing, Wei Ge, Yongli Xiao, Jinghai Li (2008); Arratia, Duong, Muzzio, Godbole and Reynolds (2006); Kwapinska, Saage and Tsotsas (2008); Bertrand, Leclaire and Levecque (2005); Gudin, Kano and Saito (2007)]. All these studies are characterised by one-dimensional motion of the vessel geometry around one-fixed axis. In this paper the complicated three-dimensional motion of a vessel located within the Turbula mixer chamber has been modelled.

The improved Graphical User Interface GUI of commercial DEM codes and the readily available computational power allow complex mixing systems to be simulated. There is a need to explore the ability of DEM simulations to provide an insight into mixing mechanisms in equipment in which flow is difficult to observe, let alone measure, on the granular scale.

The Turbula mixer (Willy A. Bachofen AG Maschinenfabrik, Basel, Switzerland), shown in Fig. 1, is a laboratory scale mixer used in the development or testing of new products. It has a capacity of 2 L and can hold any form of container. The rotational speed can be varied from 22 to 100 *rpm*. The mixing vessel, located in the mixer chamber, is subjected to intensive, periodically pulsating movements, which simulate the pattern of agitation achieved by manual shaking [Sommier, Porion, Evesque, Leclerc, Tchoreloff and Couarraze (2001)]. This extremely complicated movement is composed of two rotations of the container and a horizontal translation. In addition to the traditional principal motions of rotation and translation there is a third fundamental motion of inversion based on the Schatz inversion principle [Schatz (1933)]. This inversion subjects the contents of the mixing container to two alternating, rhythmic pulsating motions, which causes the material to be swept by

an intense “turbulence” [Sommer (2000)]. Experimental evaluation of the Turbula to understand the mixing mechanisms are difficult to carry out due to its complicated motion. The commercial EDEM package is employed in this work since it is capable of managing complicated geometries and complicated dynamics. The aim is to assess whether DEM can deliver fundamental mechanistic understanding of the granular flow behaviour in this mixer and provide a generic methodology for DEM experimentation.

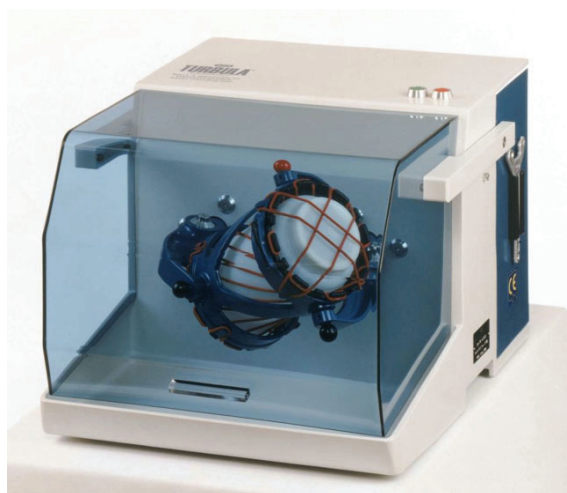


Figure 1: Turbula T2F shaker-mixer (reproduced with the kind permission of Willy A. Bachofen AG Switzerland).

Despite its widespread use as a laboratory scale blender in the catalyst and pharmaceutical industries, only a few mixing studies using the Turbula have been reported in the literature. For example, Magnetic Resonance Imaging (MRI) has been used to study the mixing of binary, free flowing, non-cohesive, sugar beads [Sommer, Porion, Evesque, Leclerc, Tchoreloff and Couarraze (2001)]. The rate of mixing of particles with monomodal and bimodal size distributions was quantified using a segregation index. Experiments revealed that segregation appeared as soon a particle diameter ratio is present.

In this work an attempt to model the motion of particles in the mixer has been carried out using DEM. This is part of a larger piece of work in which the motion of the modelled particles is compared with real experimental data in order to validate the model. In this paper, the Turbula motion was directly measured using Multiple Positron Emission Particle Tracking (Multiple-PEPT) and described

mathematically for use in DEM.

2 Experimental: Turbula motion measurement

In order to determine the Turbula motion the Multiple Positron Emission Particle Tracking (Multiple-PEPT) technique was employed. [Yang, Fan, Bakalis, Parker and Fryer (2008)] have shown that the PEPT technique can be used to track, with good accuracy, three particles at the same time. In one application it was shown that the rotational and translational motion of a solid body can be reconstructed from three positron emitting tracers mounted at fixed and known locations on the surface of the solid.

In the following paragraphs the basic PEPT principles and the specific details of Multiple-PEPT are presented.

2.1 Positron Emission Particle Tracking (PEPT)

Positron emission particle tracking is a non-invasive technique for following the motion in three dimensions, of a radioactive tracer particle. The technique has been developed at the University of Birmingham [Hawkesworth, Parker, Fowles, Crilly, Jefferies and Jonkers, G. (1991); Parker, Allen, Benton, Fowles, McNeil, Tan and Beynon (1997); Parker, Forster, Fowles and Takhar (2002); Fan, Parker and Smith (2006)].

The schematic set-up for PEPT camera is shown in Fig. 2, and it consists of a pair of parallel detectors, a radioactive tracer and an algorithm for the calculation of the particle location. The tracer particle is labelled with a radionuclide, which decays by β^+ decay resulting in the emission of a positron. Each positron rapidly annihilates with an electron, producing a pair of back-to-back 511keV γ -rays, which are then detected by the two position-sensitive detectors.

Each detector has an active area of $500 \times 400 \text{ mm}^2$, mounted on either side of the field of view.

The technique has been employed in numerous applications as extensively reported in literature in different occasions. [Seville, Ingram, Fan and Parker (2009)] presented an extended summary of different case studies and applications for PEPT. [Jones and Bridgwater (1998)] employed PEPT to determine when a particle moves between inter-plough regions within a ploughshare mixer. [Ding, Seville, Forster and Parker (2001)] characterised the characteristic rolling mode for a rotating drum operating at low and medium speed and the solid motion in the active region was investigated. [Ingram, Hausard, Fan, Parker, Seville, Finn and et al. (2007)] used a modular camera to understand particle motion in a 750mm diameter pressurised fluidised bed pilot plant reactor on an industrial plant. [Wildman, Blackburn, Ben-

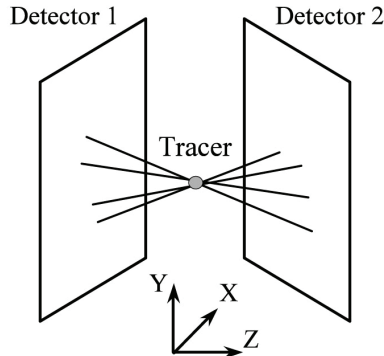


Figure 2: Schematic representation of PEPT (Positron Emission Particle Tracking) camera.

ton, McNeil and Parker (1999)] demonstrated the plug flow of the paste inside the barrel and die land region during extrusion by the analysis of particle speed.

One drawback of the standard PEPT technique is that it is only capable of following a single tracer at any one time. In some situations, such as for mixing of multiple component particle systems, it would be beneficial to track more than one particle in order to have a better understanding of the mixing mechanisms. For this reason the Multiple-PEPT technique has been developed [Yang, Fryer, Bakalis, Fan, Parker and Seville (2007)].

2.2 Multiple Positron Emission Particle Tracking (Multiple-PEPT)

The Multiple-PEPT is a technique that was developed from the single particle tracking PEPT. With this technique it is possible to follow with reasonable accuracy up to three multiple particles simultaneously through a considerable thickness of surrounding material. Since each tracer will emit the same gamma photons the tracers are distinguished by labelling with different levels of activity and using a statistical approach to home in the centres of emission. The technique for particle identification, location calculation and time reconstruction for multiple particles has been presented recently by [Yang, Fryer, Bakalis, Fan, Parker and Seville (2007)].

2.3 Experimental set-up for the motion measurement

Fig. 3 shows the schematic experimental set-up for the Turbula motion measurements. Three tracers were precisely fixed on the Turbula shaft at location points P_A , P_C and P_D .

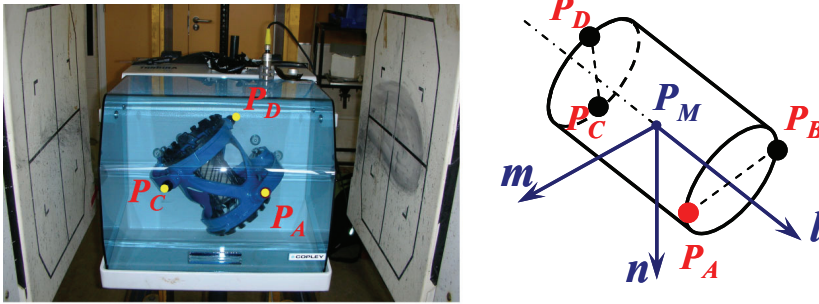


Figure 3: Schematic representation of the experimental measurement of the Turbula motion by PEPT.

The tracers were Zeolite particles from a sample with a d_{50} of $323\mu m$. They were labelled with ^{18}F with different initial radioactivity: tracer 1 (point \mathbf{P}_A): $880\mu\text{Ci}$; tracer 2 (point \mathbf{P}_C): $596\mu\text{Ci}$; tracer 3 (point \mathbf{P}_D): $395\mu\text{Ci}$. During measurements the three tracers were tracked over several periods of the Turbula rotation to obtain an accurate trajectory for each of the three points from which the complete motion of the Turbula would be determined.

2.4 Translational and rotational motion reconstruction

The translational and rotational motion the Turbula can be reconstructed by knowing the position over time of the three points that are rigidly attached to the moving shaft of the mixer. Fig. 4 reports the positions of points \mathbf{P}_A , \mathbf{P}_C and \mathbf{P}_D in Cartesian coordinates with respect to the camera coordinate versus the shaft angle at 23rpm (rotation period 2.613sec). This cycle reported in Fig. 4 has been used for the motion reconstruction.

The time interval between PEPT locations is variable as can be seen in Fig. 4. This can be attributed to the PEPT algorithm and the way that data is used to compute tracer location: the algorithm uses a fixed number of photon pairs to compute each location – the frequency of these can be variable depending on where the particles are in the field of view. Furthermore, the algorithm rejects computed locations that have high uncertainty – this can give apparent gaps in the data. The latter is more of an issue with multiple particle tracking due to the inherent corrupting effect of multiple sources of identical gamma photons. In order to reconstruct a more useable motion for DEM the data is interpolated and filtered at a constant time step.

Considering Fig. 4, where the tracked locations are fixed relative to each other

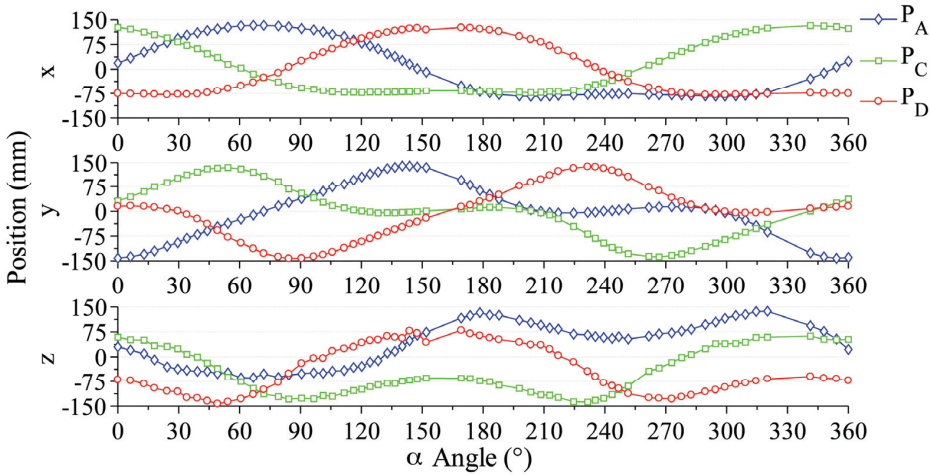


Figure 4: Measured position x,y,z for the tracers fixed at position \mathbf{P}_A , \mathbf{P}_C and \mathbf{P}_D by Multiple-PEPT at $23rpm$ for one shaft rotation.

and correspond to the pivoting points of the vessel holder, some symmetry in the trajectories is apparent. Since the central axis of the machine is horizontal, each tracked point follows the same trajectory in the transverse (x,y) plane out of phase by a multiple of 90° from the other points. Motion in the horizontal (z) direction is slightly more complex. Points at the same end of the vessel holder follow the same path, but out of phase by 180° . The trajectories of points at opposite ends are also out of phase (by 90°) but, in addition there is a displacement (related to the length of the Turbula) and an inversion (mirror image). These transformations can be applied as shown in Figure 5.

From Fig. 5 it can be seen that the three measured points follow the same trajectories. There are some small differences due to the location error for the tracers' location in the measurement. It can be concluded though that to minimize the error, and obtain a better motion reconstruction into DEM, only the trajectory of a single point \mathbf{P}_A need be used, as this is the most intense source. Subsequent experiments used a single particle on point \mathbf{P}_A . The trajectories for the other \mathbf{P}_B , \mathbf{P}_C and \mathbf{P}_D points are inferred from point \mathbf{P}_A as described above. Note that the point \mathbf{P}_B is on the opposite knob with reference to the point \mathbf{P}_A in Fig. 3.

The position and orientation of the Turbula can be defined uniquely by the position vector of its centroid, \mathbf{P}_M , a unit vector along its axis, \mathbf{l} , and a radial unit vector \mathbf{m}

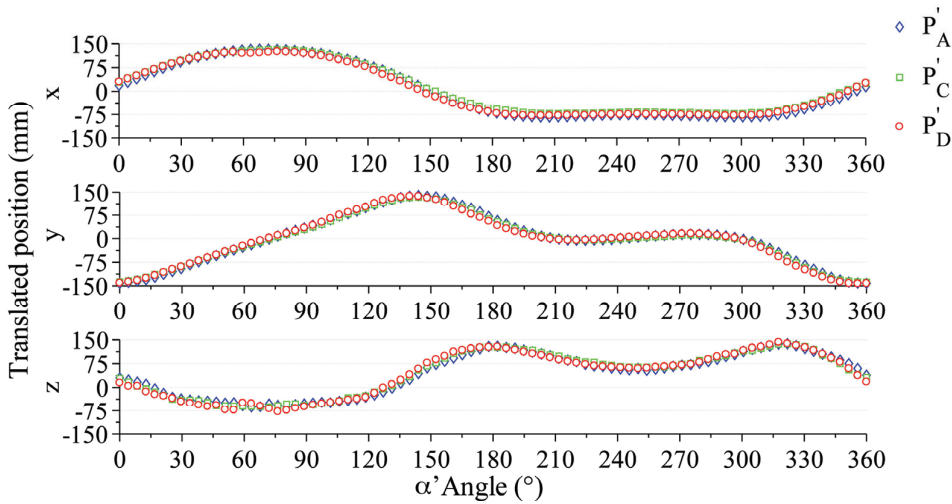


Figure 5: x,y,z positions for point \mathbf{P}_A , \mathbf{P}_C' and \mathbf{P}_D' from Multiple-PEPT at 23rpm for one shaft rotation.

as shown in figure 3 above. \mathbf{P}_M, \mathbf{l} and \mathbf{m} are related to $\mathbf{P}_A, \mathbf{P}_B, \mathbf{P}_C$ and \mathbf{P}_D by:

$$\mathbf{P}_M = \left(\frac{\mathbf{P}_A + \mathbf{P}_B + \mathbf{P}_C + \mathbf{P}_D}{4} \right) \tag{1}$$

$$\hat{\mathbf{l}} = \frac{\left[\left(\frac{\mathbf{P}_A + \mathbf{P}_B}{2} \right) - \left(\frac{\mathbf{P}_C + \mathbf{P}_D}{2} \right) \right]}{\left\| \left(\frac{\mathbf{P}_A + \mathbf{P}_B}{2} \right) - \left(\frac{\mathbf{P}_C + \mathbf{P}_D}{2} \right) \right\|} = (\hat{l}_1, \hat{l}_2, \hat{l}_3) \tag{2}$$

$$\hat{\mathbf{m}} = \frac{\left[\mathbf{P}_A - \left(\frac{\mathbf{P}_A + \mathbf{P}_B}{2} \right) \right]}{\left\| \mathbf{P}_A - \left(\frac{\mathbf{P}_A + \mathbf{P}_B}{2} \right) \right\|} = (\hat{m}_1, \hat{m}_2, \hat{m}_3) \tag{3}$$

The components of \mathbf{P}_M, \mathbf{l} and \mathbf{m} are periodic and can therefore be expressed as Fourier series of the form:

$$f(t) = \frac{1}{2} a_0 + \sum_{n=1}^{\infty} [a_n \cos n\omega t + b_n \sin n\omega t] \tag{4}$$

where a_0, a_n and b_n are Fourier coefficients and T is the rotational period, 2.613sec at 23rpm.

Satisfactory approximations can be obtained by using only a few terms in the Fourier series; the original and reconstructed values of the components of \mathbf{l} and \mathbf{m} are compared in Fig. 6 and 7.

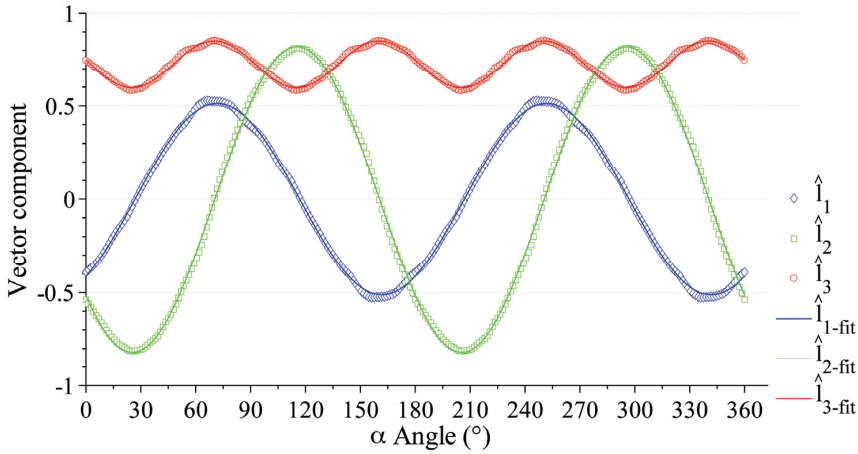


Figure 6: Components for the unit vector \hat{l} .

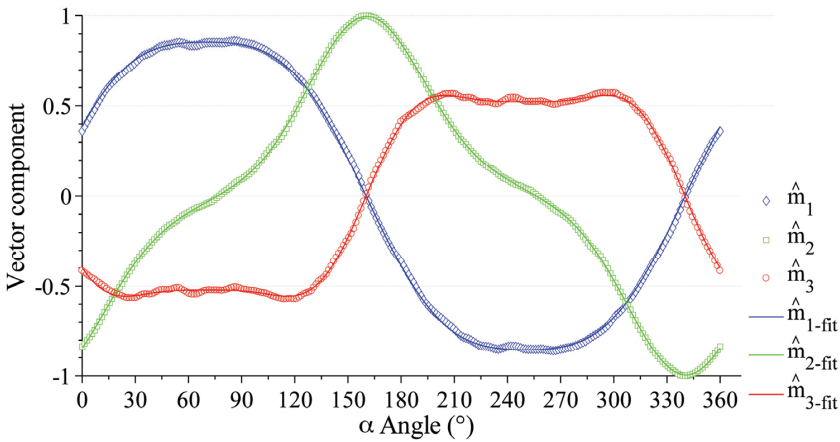


Figure 7: Components for the unit vector \hat{m} .

The EDEM software allows the motion of a rigid solid body to be defined as a superposition of translational and rotational movements as reported in Fig. 8. It does this by approximating the smooth motion of the Turbula as a succession of discrete timesteps during which the translational and angular velocities are constant. In this first attempt of modelling the Turbula mixer, a motion timestep of $t_{step} = 0.01 \text{ sec}$ has been chosen since the EDEM software is limited in how many total superimposed

translations and rotations can be defined due to computational limitations. Physically this corresponds to subjecting the contents of the Turbula to a succession of small impulsive blows, but the time step has been chosen sufficiently small that this should have a negligible effect on the solution.

Translational velocity:

```
<linear_translation name="ti" t_start="tI+(i-1)·tstep" t_end="tI+i·tstep"
start_vel_x="v1i" start_vel_y="v2i" start_vel_z="v3i"
```

.....

Rotational velocity:

```
<linear_rotation name="ri" t_start="tI+(i-1)·tstep" t_end="tI+i·tstep"
start_angvel_x="ω1i" start_angvel_y="ω2i" start_angvel_z="ω3i"
```

Figure 8: Coding translations and rotations into DEM.

with $i = 1 : n$, where n is the desired number of translation and rotations that will give the total motion duration. t_i is the actual time at which the linear translational velocity (v_{1i}, v_{2i}, v_{3i}) and rotational velocity (w_{1i}, w_{2i}, w_{3i}) are applied.

The Gibbs-Rodrigues representation [see e.g. Peterson (2003)] provides a convenient way to calculate w_i . In this a rotation by an angle θ about an axis defined by a unit vector \mathbf{n} is represented by a vector $\mathbf{r} = \mathbf{n} \tan(\theta/2)$.

The rotation from orientation \mathbf{l}, \mathbf{m} at time t to new orientation \mathbf{l}', \mathbf{m}' at time $t'=t+t_{step}$ is given by:

$$r_i = \frac{\sum_{j=1}^3 \sum_{k=1}^3 \epsilon_{ijk} l_j l'_k + \gamma(l_i + l'_i)}{\sum_{k=1}^3 l_k (l_k + l'_k)} \tag{5}$$

where ϵ_{ijk} is the unit antisymmetric tensor and γ is calculated as follows:

$$\gamma = - \frac{\sum_{i=1}^3 \sum_{j=1}^3 \sum_{k=1}^3 \epsilon_{ijk} l_j l'_k (m_i - m'_i)}{\sum_{i=1}^3 (l_i + l'_i) (m_i - m'_i)} \tag{6}$$

The average angular velocity over this time step is therefore given by:

$$\omega = \frac{\theta}{t' - t} \cdot \frac{\mathbf{r}}{\|\mathbf{r}\|} = (\omega_1, \omega_2, \omega_3) \tag{7}$$

Figure 9 shows the calculated components of the angular velocity as a function of time.

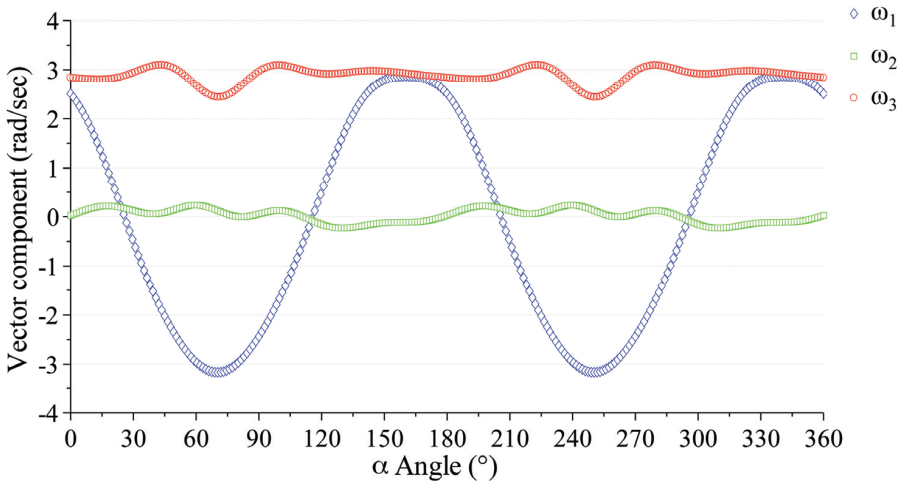


Figure 9: Components of the angular velocity ω .

EDEM imposes ω about the origin of the coordinate system rather than the centroid of the Turbula, so the translational velocity necessary to match the movement of the centroid is given by:

$$\mathbf{v} = \dot{\mathbf{P}}_{\mathbf{M}} - \omega \wedge \mathbf{P}_{\mathbf{M}} = (v_1, v_2, v_3) \tag{8}$$

Again the components are reported in Fig. 10.

The tabulated values of \mathbf{v} and ω at each timestep are used for importing the motion into DEM. The experimental measurement of the motion tracking has been conducted at 23rpm, but can easily be scaled to other speeds by modifying \mathbf{v} and ω .

3 Numerical model DEM

3.1 DEM model set-up

Discrete Element Modelling (DEM) is a numerical tool that can be used to model particulate material as an assembly of discrete particles, which interact with each other and with any other solid body such as equipment geometries.

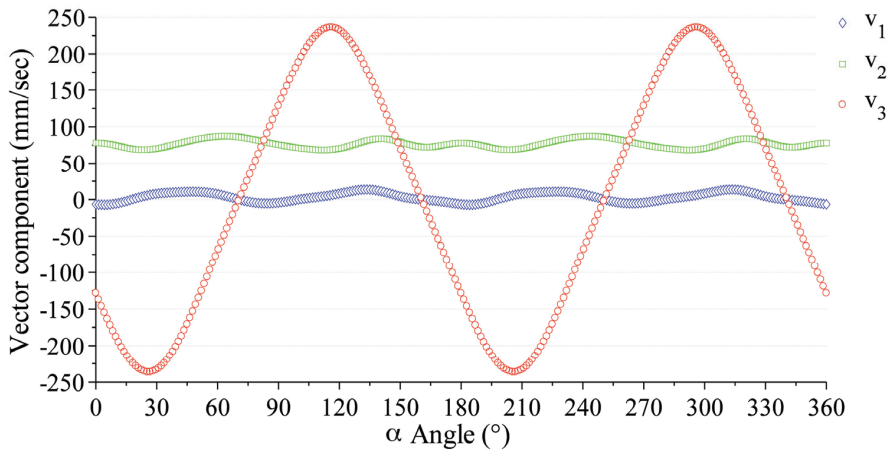


Figure 10: Components of the linear velocity v .

There are plenty of examples of DEM reported in the literature addressing the diversity of granular behaviour such as separation, mixing, material transport, comminution, agglomeration, material storage, particle packing and fluid-particulate flow. A brief overview of selected DEM applications are given as follows.

DEM simulations of the three dimensional motion of particles in powder mixers have been studied by several authors. Improvements in mixing rate from the incorporation and design of baffle geometry [Muguruma, Tanaka, Kawatake and Tsuji (1997)] and achieving perfect mixing by optimizing mixing time and mixing number for different drum diameters, rotational frequencies, drum loadings and average particle diameters [Kwapinska, Saage, and Tsotsas (2006)] are two examples of studies using rotating cylinders. The more complex geometry of V-mixers have been simulated with results compared to experimental data on monosized 3 mm glass beads obtained using Positron Emission Particle Tracking (PEPT) [Kuo, Knight, Parker and Seville (2005)]. They show the choice of DEM input parameters can influence the simulation results in terms of particle velocity, exchange rate between the two arms of the mixer, circulation time and dispersion coefficient. DEM simulations and experimental results on a double-cone blender and V-mixer by [Moakher, Shinbrot and Muzzio (2000)] show that convection is the dominant mixing mechanism and axial dispersion is less effective. DEM simulations have been used in conjunction with experimental data to predict the non-first order breakage rate of dry coarse particles in a ball mills [Tavares and Carvalho (2009)]. By combining DEM simulations of the distribution of stressing energies

in the mill with the distribution of particle fracture energies obtained by single particle impact test. DEM simulations and experimental results have also been used to study wet milling processes. The experimental grinding rate constant for a gibbsite powder suspension has been correlated with the specific impact energy of the milling media simulated by DEM [Gudin, Turczyn, Mio, Kano and Saito (2006)]. This correlation allows the prediction of the grinding rate constant by using the collision impact energies obtained from the DEM simulations under different operational conditions. The motion of polygonal and superquadric irregular particles was studied under turbulent flow along a pipe with suction action by coupling the Lattice Boltzmann Method (LBM) and DEM [Han, Feng and Owen (2007)]. Work by [Scholtès, Chareyre, Nicot and Darve (2009)] demonstrated the effect of capillary forces on the friction of a granular assembly using by Young-Laplace equation. It was shown that the inter-particle menisci contribute to the granular material resistance by increasing normal forces at contact points. One part of the tableting process is die filling which is powder particles flowing into a die and displacing air from it. DEM has been combined with Computational Fluid Dynamics (CFD) by [Guo, Wu, Kafui and Thornton (2010)] to take into account the presence of air for a binary mixture in different die geometries for stationary and moving shoes. DEM has also been used to evaluate the packing structure of particles. Good agreements were found in terms of coordination number (CN) and radial distribution function (RDF) between the simulations and X-ray tomography results for monodisperse acrylic spheres [Aste, Di Matteo and Tordesillas (2007)]. Three-dimensional maps of the internal structure of dense random packings have been simulated and validated by X-ray tomography for glass ballotini and spherical micronised cellulose particles by [Fu, Dutt, Bentham, Hancock, Cameron and Elliott (2006)]. A digital DEM algorithm has been presented by [Xu, Jia, Williams, Stitt, Nijemeisland, Bachir, Sederman and Gladden (2008)] to represent the packing of pellets with complicated shapes. The digital DEM model is based on a digitised representation of the pellet and the voxel contact forces acting on the pellet. Simulations of the packing of cylindrical pellets in a tube were in good agreement, in terms of packing density and spatial statistic, with Magnetic Resonance Imaging (MRI) experimental results.

An advantage of DEM modelling is the fact that useful information can be directly extracted from the simulation, which is otherwise difficult to obtain experimentally. For example, the number of contacts between particles can be obtained or the observation of particle velocity fields can reveal the mixing mechanisms that control the material dynamics inside a mixer. A disadvantage of DEM is that real particle systems with millions of particles with irregular shapes cannot be simulated efficiently using the current state of the art. At the moment computational performance lim-

its the usage of the DEM. However, developments in computational power should resolve this problem in the future.

The DEM version employed in this work is a commercially available package provided by DEM-Solutions (EDEM version 2.0).

3.2 DEM numerical model

In the DEM numerical algorithm the total force acting on each particle is calculated at each timestep and hence the translation and rotation motion can be described by integrating the Newton's equations of motion.

In this work only the gravitational and contact force during collision are considered. Therefore the Newton's equations for a particle i with radius R_i and mass m_i assume the following form:

$$m_i \frac{d\mathbf{v}_i}{dt} = \sum_j^n (\mathbf{F}_{ij}^n + \mathbf{F}_{ij}^t) + m_i \mathbf{g} \quad (9)$$

$$I_i \frac{d\boldsymbol{\omega}_i}{dt} = \sum_j^n (\mathbf{R}_i \times \mathbf{F}_{ij}^t - \boldsymbol{\tau}_{ij}^r) \quad (10)$$

where $\mathbf{v}_i, \boldsymbol{\omega}_i$ are the i particle translational speed and rotational speed. $\boldsymbol{\tau}_{ij}^r$ is the torque due to rolling friction between particle i and j . \mathbf{F}_{ij}^n and \mathbf{F}_{ij}^t are the normal and the tangential contact forces due to collisions between particle i and j .

A contact model is required to evaluate the contact force terms between each individual particle. The contact detection is the most computationally time-demanding operation.

The modified Hertz Mindlin (no-slip) contact model provided in the EDEM software has been used in this work. This contact model is an extension of the Hertz normal elastic contact model and the Mindlin contact model in the tangential direction; the energy during collision is dissipated through a viscous damping coefficient and friction between the particles [Raji and Favier (2003)].

In Table 1 lists the parameters used in the present work are reported. Parameter marked with an asterisk * are the same as those used in DEM work to model glass beads [Yang, Zou, and Yu (2003)]. The remaining physical parameters are assumed.

A cylindrical vessel with a diameter of 45mm and length 80mm was partially filled with spherical particles. The movement of the vessel simulated at five speeds is reported in Table 2 for five different cases. In all simulations two different particle sizes, with the same mass fraction, were used. The particle diameter ratio is defined

Table 1: EDEM simulation parameters.

Parameter	Base Value
Particle diameter, d [mm]	2 – 1.4
Particle density [g/cm^3]	2.5
Particle shear modulus G [Pa]	2×10^6
Poisson's ratio	0.3
Vessel density [g/cm^3]	1.2
Vessel shear modulus G [Pa]	3×10^9
Vessel Poisson's ratio	0.3
Particle-particle static friction coefficient	0.5 *
Particle-particle rolling friction coefficient	0.01 *
Particle-vessel static friction coefficient	0.35
Particle-vessel rolling friction coefficient	0.005
Particle-particle restitution coefficient	0.73 *
Particle-vessel restitution coefficient	0.73 *
Cohesivity factors	0

as:

$$R = \frac{d_{Particle_typeA}}{d_{Particle_typeB}} \quad (11)$$

In this work in order to simulate fewer particles and to reduce the simulation time a particle diameter ratio R of 1.4 has been used rather than the 2.8 used by Sommier, Porion, Evesque, Leclerc, Tchoreloff and Couarraze (2001).

Table 2: EDEM simulations conditions.

Case	Particle diameter (mm) (Number of particles)	Fill %	R	Speed (rpm)
1	2 (4500) - 1.4 (13100)	≈ 50	1.4	23
2	2 (4500) - 1.4 (13100)	≈ 50	1.4	34
3	2 (4500) - 1.4 (13100)	≈ 50	1.4	46
4	2 (4500) - 1.4 (13100)	≈ 50	1.4	57
5	2 (4500) - 1.4 (13100)	≈ 50	1.4	69

4 Results: DEM simulations

The aim of this work is to model the dynamic of the Turbula mixer in order to describe the mixing behaviour within the vessel. In this paragraph preliminary results and a qualitative comparison with data from literature is reported. In Fig. 11.a the initial particle loading pattern is shown, the colours represent the 2 types of particles (red for 1.4mm diameter and blue for 2mm diameter particles). In Fig. 11.b a section of the vessel is reported. The final particle pattern with a concentration of small particles in the middle of the particle bed can be observed.

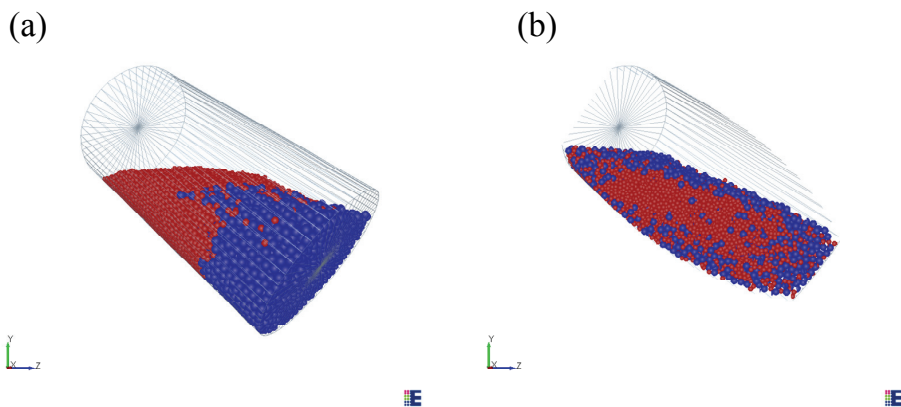


Figure 11: (a) Initial loading pattern and (b) final pattern after 15 rotations for monodisperse and bidisperse simulations at 23rpm and $R=1.4$.

4.1 Mixing rate

The degree of mixing and the time needed to achieve an acceptable mixing can be predicted by simulations. In literature different methods for defining the mixing or segregation time have been proposed. For example [Arratia, Duong, Muzzio, Godbole and Reynolds, 2006] employed a segregation index based on the analysis of the relative standard deviation of the concentration in n samples. [Kwapinska, Saage, Tsotsas (2006); Geng, Yuan, Yan, Luo, Wang, Li and Xu (2009)] recorded the number of contacts during mixing and the bed of particles was assumed to be uniform when the number of contacts between the two fractions starts to randomly fluctuate around a constant value. In this work a segregation parameter, proposed by [Stambaugh, Smith, Ott and Losert (2004)], is employed. The definition of this index is different than the one based in voxel statistical analysis and used in the MRI

measurements of [Sommier, Porion, Evesque, Leclerc, Tchoreloff and Couarraze (2001)]. However similar trends should be expected regarding mixing behaviour. The segregation index S' is defined as:

$$S' = \frac{C_{AA}}{C_{AA} + C_{AB}} + \frac{C_{BB}}{C_{BB} + C_{AB}} \tag{12}$$

where C_{ij} is the total number of contact between particles of type i and particles of type j (with i and j equal to A or B). This segregation index has the advantage of symmetry under interchange of particle type and equal weighting of the segregation of each type. The segregation index assumes the values between $0 \leq S' \leq 2$, and in case of random mixtures it assumes the value of $S' = 1$. $S' = 2$ and $S' = 0$ in case of complete segregated system and perfectly ordered system. An example of DEM result for the segregation index S' against time showing the rate asymptotic degree of segregation is showed in Fig. 12.

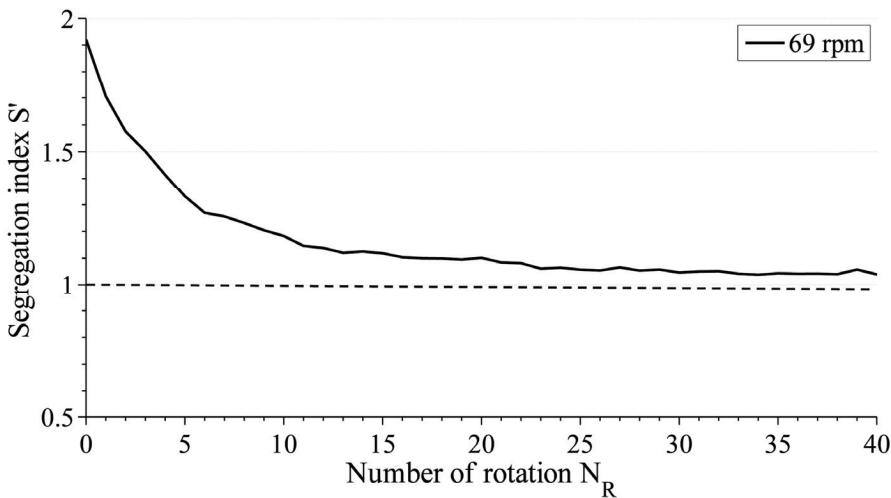


Figure 12: DEM segregation index against time 69rpm.

It is well known that particles of sufficiently different sizes may segregate [Arratia, Duong, Muzzio, Godbole and Reynolds (2006)], even in simple shear flows. Here, we investigate segregation using a bi-disperse collection of particles with a size ratio of 1.4.

[Sommier, Porion, Evesque, Leclerc, Tchoreloff and Couarraze (2001)] observed that segregation increases when the particle diameter ratio differs than 1. They observed high concentrations of large particles along the inner wall of the container

and on the free surface. This can be observed in Fig. 11.b as results from the simulation.

4.2 Influence of rotational speed ($R \neq 1$)

[Sommier, Porion, Evesque, Leclerc, Tchoreloff and Couarraze (2001)] also showed that the segregation index decreases when the rotational speed increases but that even at the highest speeds the system remains segregated.

In Fig. 13a the segregation index from [Sommier, Porion, Evesque, Leclerc, Tchoreloff and Couarraze (2001)] is reported as function of rotation speed in the case when $R=2.8$. In Fig. 13b the segregation index determined from the DEM simulation, for $R=1.4$ at steady state, is reported as function of rotation speed. Good qualitative agreements can be observed between the experimental results and the DEM simulations. The increase of rotational speed leads to an improvement in the quality of mixing.

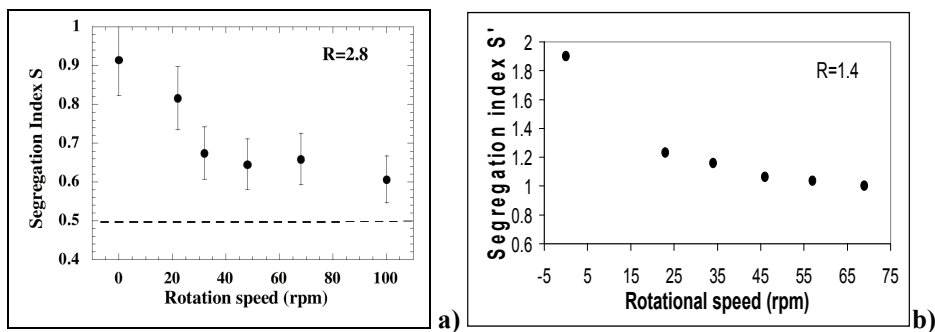


Figure 13: Steady state segregation index versus rotation speed. a) Experiments from [Sommier, Porion, Evesque, Leclerc, Tchoreloff and Couarraze (2001)]. b) DEM simulations, value at steady state.

5 Conclusions

The Positron Emission Particle Tracking has been used to measure the Turbula motion. It has been shown that the Multiple-PEPT technique can track three particles and it has been used to understand the Turbula motion. The technique has been employed to calculate both the translational and rotational motions of a solid body of the mixer to recreate the motion into the DEM software.

A first attempt of discrete element modelling of the three-dimensional motion of particles in a Turbula mixer was carried out by DEM. The results have been presented and discussed in terms of segregation index.

Good qualitative agreements have been found between DEM simulations and experimental data by [Sommier, Porion, Evesque, Leclerc, Tchoreloff and Couarraze (2001)]. More experimental investigations are necessary in order to properly validate the DEM model. Future work will be carried out by comparing DEM simulations and PEPT mixing experiments on glass beads and catalyst support material. In addition an exploration of the dominant mixing mechanisms in the mixer is being carried out.

Acknowledgement: MM would like to acknowledge the EU for financial support through the Framework 6 Marie Curie Action "NEWGROWTH", contract number MEST-CT-2005-020724, Johnson Matthey Plc for funding and supporting this research.

References

- Arratia, P. E.; Duong, N.; Muzzio, F.J.; Godbole, P.; Reynolds, S.** (2006): A study of the mixing and segregation mechanisms in the Bohle Tote blender via DEM simulations. *Powder Technology*, vol. 164, no. 1, pp. 50-57.
- Aste, T.; Di Matteo, T. .; Tordesillas, A.** (Editors) (2007) Granular and Complex Materials. *World Scientific Lecture Notes in Complex Systems*, vol.8.
- Ding, Y. L.; Seville, J. P. K.; Forster, R.; Parker, D. J.** (2001): Solids motion in rolling mode rotating drums operated at low to medium rotational speeds. *Chemical Engineering Science*, vol. 56, no. 5, pp. 1769-1780.
- Cundall, P.A.; Strack, O.D.L.** (1979): A discrete numerical model for granular assemblies. *Geotechnique*, vol. 29, no. 1, pp. 47-65.
- Bertrand, F.; Leclaire, L.-A.; Levecque, G.** (2005): DEM-based models for the mixing of granular materials. *Chemical Engineering Science*, vol. 60, nb. 8-9, pp. 2517-2531.
- Fan, X.; Parker, D.J.; Smith, M.D.** (2006). Labelling a single particle for positron emission particle tracking using direct activation and ion-exchange techniques. *Nuclear Instruments and Methods in Physics Research Section A: Accelerators, Spectrometers, Detectors and Associated Equipment*, vol. 562, no.1, pp. 345-350.
- Fu, X.; Dutt, M.; Bentham, A. C.; Hancock, B.C.; Cameron, R.E.; Elliott, J.A.** (2006): Investigation of particle packing in model pharmaceutical powders using X-ray microtomography and discrete element method *Powder Technology*,

vol. 167, no. 3, pp. 134-140.

EDEM user guide (2009): EDEM Help version 2.1.1 rev 7B.

Geng, F.; Yuan, Z.; Yan, Y.; Luo, D.; Wang, H.; Li, B.; Xu, D. (2009): Numerical Simulation on Mixing Kinetics of Slender Particles in a rotary dryer. *Powder Technology*, vol. 193, no. 1, pp. 50-58.

Gudin, D.; Turczyn, R.; Mio, H.; Kano, J.; Saito F. (2006): Simulation of the movement of beads by the DEM with respect to the wet grinding process. *AIChE Journal*, vol.52, no. 10, pp. 3421–3426.

Gudin, D.; Kano, J.; Saito, F. (2007): Effect of the friction coefficient in the discrete element method simulation on media motion in a wet bead mill. *Advanced Powder Technol.*, vol. 18, no. 5, pp. 555–565.

Guo, Y.; Wu, C.-Y.; Kafui, K.D.; Thornton, C. (2010): Numerical analysis of density-induced segregation during die filling. *Powder Technology*, vol.197, no. 1-2, pp. 111-119.

Han, K.; Feng, Y.; Owen, D. (2007): Numerical simulations of irregular particle transport in turbulent flows using coupled LBM-DEM. *CMES: Computer Modeling in Engineering and Science*, vol. 18, no. 2, pp. 87–100.

Hawkesworth, M. R.; Parker, D. J.; Fowles, P.; Crilly, J. F.; Jefferies, N. L.; Jonkers, G. (1991) Nonmedical applications of a positron camera. *Nuclear Instruments and Methods in Physics Research Section A: Accelerators, Spectrometers, Detectors and Associated Equipment*, vol. 310, no. 1-2, Pages 423-434.

Ingram, A.; Hausard, M.; Fan, X.; Parker, D.J.; Seville, J. P. K.; Finn, N.; et al. (2007): 12th International Conference on Fluidization. *New Horizons in Fluidization Engineering, ECI Engineering Conference International Symposium Series*, paper 60.

Lemieux, M.; Léonard, G.; Doucet, J.; Leclaire, L.-A.; Viens, F.; Chaouki, J.; Bertrand, F. (2008): Large-scale numerical investigation of solids mixing in a V-blender using the discrete element method. *Powder Technology*, vol. 181, no. 2, pp. 205-216.

Liu, X.; Ge, W.; Xiao, Y.; Li, J. (2008): Granular flow in a rotating drum with gaps in the side wall. *Powder Technology*, vol. 182, no. 2, pp. 241-249.

Lochmann, K.; Oger, L.; Stoyan, D. (2006): Statistical analysis of random sphere packings with variable radius distribution. *Solid state science*, vol. 8, no. 12, pp. 1397-1413.

Moakher, M.; Shinbrot, T.; Muzzio, F. J. (2000): Experimentally validated computations of flow, mixing and segregation of non-cohesive grains in 3D tumbling blenders. *Powder Technology*, vol. 109, no. 1-3, pp. 58-71.

- Moysey, P.A.; Thompson, M.R.** (2005): Modelling the solids inflow and solids conveying of single-screw extruders using the discrete element method. *Powder Technology*, vol. 153, no. 2, pp. 95-107.
- Muguruma, Y.; Tanaka, T.; Kawatake, S.; Tsuji, Y.** (1997): Discrete particle simulation of a rotary vessel mixer with baffles. *Powder Technology*, vol. 93, no. 3, pp. 261-266.
- Jones, J. R.; Bridgwater, J.** (1998): A case study of particle mixing in a ploughshare mixer using Positron Emission Particle Tracking. *International Journal of Mineral Processing*, vol. 53, no. 1-2, pp. 29-38.
- Kuo, H. P.; Knight, P. C.; Parker, D. J.; Tsuji, Y.; Adams, M. J.; Seville, J. P. K.** (2002): The influence of DEM simulation parameters on the particle behaviour in a V-mixer. *Chemical Engineering Science*, vol. 57, no. 17, pp. 3621-3638.
- Kuo, H.P.; Knight, P.C.; Parker, D.J.; Seville J.P.K.** (2005): Solids circulation and axial dispersion of cohesionless particles in a V-mixer. *Powder Technology*, vol. 152, no. 1-3, pp. 133-140.
- Kwapinska, M.; Saage, G.; Tsotsas, E.** (2006): Mixing of particles in rotary drums: A comparison of discrete element simulations with experimental results and penetration models for thermal processes. *Powder Technology*, vol. 161, no. 1, Pages 69-78.
- Kwapinska, M.; Saage, G.; Tsotsas, E.** (2008): Continuous versus discrete modelling of heat transfer to agitated beds. *Powder Technology*, vol. 181, no. 3, pp. 331-342.
- Parker, D. J.; Allen, D. A. ; Benton, D. M. ; Fowles, P. ; McNeil, P. A.; Tan, Min; Beynon, T. D.** (1997). Developments in particle tracking using the Birmingham Positron Camera. *Nuclear Instruments and Methods in Physics Research Section A: Accelerators, Spectrometers, Detectors and Associated Equipment*, vol. 392, no. 1-3, 21 June 1997, pp. 421-426.
- Parker, D. J.; Forster, R. N.; Fowles, P.; Takhar, P. S.** (2002) Positron emission particle tracking using the new Birmingham positron camera. *Nuclear Instruments and Methods in Physics Research Section A: Accelerators, Spectrometers, Detectors and Associated Equipment*, vol. 477, no. 1-3, pp. 540-545.
- Raji, A. O.; Favier, J. F.** (2004) Model for the deformation in agricultural and food particulate materials under bulk compressive loading using discrete element method. I: Theory, model development and validation. *Journal of Food Engineering*, vol. 64, no. 3, pp. 359-371.
- Seville, J.P.K.; Ingram, A.; Fan, X.; Parker, D.J.** (2009): Chapter 4 Positron Emission Imaging in Chemical Engineering. *Advances in Chemical Engineering*,

vol. 37, pp. 149-178.

Schatz, P. (1933) Deutsches Reichspatent Nr. 589 452 in *Der allgemeinen Getriebeklasse*. US Patent Nr. 2 302 804 (1942).

Scholtès, L.; Chareyre, B.; Nico, F.; Darve, F. (2009): Discrete Modelling of Capillary Mechanisms in Multi-Phase Granular Media. *CMES: Computer Modelling in Engineering and Science*, vol. 52, no. 3, pp. 297-318.

Sommier, N.; Porion, P.; Evesque, P. (2000) Mixing and Segregation Processes in Turbula Blender. *Material Research Society Symposium Proceedings*, vol. 627.

Sommier, N.; Porion, P.; Evesque, P.; Leclerc, B.; Tchoreloff, P.; Couarraze, G. (2001): Magnetic resonance imaging investigation of the mixing-segregation process in a pharmaceutical blender. *International Journal of Pharmaceutics*, vol. 222, no. 2, pp. 243-258.

Stambaugh, J.; Smith, Z.; Ott, E.; Losert, W. (2004): Segregation in a monolayer of magnetic spheres. *Physical review*, vol. 70, pp. 031304.

Tavares, L. M.; Carvalho, R. M. (2009): Modeling breakage rates of coarse particles in ball mills. *Minerals Engineering*, vol. 22, no. 7-8, pp. 650-659.

Xu, C.; Jia, X.; Williams, R.A.; Stitt, E.H.; Nijemeisland, M.; El-Bachir, S.; Sederman, A.J.; Gladden, L. F. (2008): Property predictions for packed columns using random and distinct element digital packing algorithms. *CMES: Computer Modelling in Engineering and Sciences*, vol. 23, no. 2, pp. 117-125.

Yang, Z.; Fryer, P.J.; Bakalis, S.; Fan, X.; Parker, D.J.; Seville, J.P.K (2007): An improved algorithm for tracking multiple, freely moving particles in a Positron Emission. *Particle Tracking system Nuclear Instruments & Methods in Physics Research Section A, Accelerators Spectrometers Detectors and Associated Equipment*, vol. 577, no. 3, pp. 585-594.

Yang, Z.; Fan, X.; Bakalis, S.; Parker, D.J.; Fryer, P.J. (2008): A method for characterising solids translational and rotational motions using Multiple-Positron Emission Particle Tracking (Multiple-PEPT). *International Journal of Multiphase Flow*, vol. 34, no. 12, pp. 1152-1160.

Yang, R. Y.; Zou, R. P.; Yu, A. B. (2003): Microdynamic analysis of particle flow in horizontal rotating drum. *Powder Technology*, vol. 130, no. 1-3, pp.138-146.

Wildman, R. D.; Blackburn, S.; Benton, D. M.; McNeil, P. A.; Parker, D. J. (1999): Investigation of paste flow using positron emission particle tracking. *Powder Technology*, vol. 103, no. 3, pp. 220-229.

Wu, C.-Y. (2008): DEM simulations of die filling during pharmaceutical tableting, *Particuology*, vol. 6, no. 6, pp. 412-418.